[13] Luke, Y. L. and Ufford, D., "Concerning a Definite Integral," *Journal of the Aeronautical Sciences*, Vol. 18, No. 7, July 1951, pp. 429–430.

[14] Filotas, L. T., "Response of Finite Wings to Sinusoidal Gusts or Vertical Oscillations," *Transactions of the Canadian Aeronautics and Space Institute*, Vol. 3, No. 1, March 1970, pp. 51–54.

[15] Sears, W. R., "Some Aspects of Non-Stationary Airfoil Theory and Its Practical Application," *Journal of the Aeronautical Sciences*, Vol. 8, No. 3, March 1941, pp. 104–108.

[16] Watson, G. N., *A Treatise on the Theory of Bessel Functions*, 2nd ed., Cambridge University Press, 1966, pp. 436.

[17] Filotas, L. T., "Theory of Airfoil Response in a Gusty Atmosphere: Part I. Aerodynamic Transfer Function," Rept. 139, 1969, Institute for Aerospace Studies, University of Toronto, Toronto, Ontario, Canada.

[18] Murrow, H. N., Pratt, K. G., and Drischler, J. A., "An Application of a Numerical Technique to Lifting-Surface Theory for Calculation of Unsteady Aerodynamic Forces Due to Continuous Sinusoidal Gusts on Several Wing Planforms at Subsonic Speeds," TN D-1501, 1963, NACA.

[19] Miles, J. W., "On the Compressibility Correction for Subsonic Unsteady Flow," *Journal of the Aeronautical Sciences*, Vol. 17, No. 3, March 1950, pp. 181–182.

JUNE 1971 J. AIRCRAFT VOL. 8, NO. 6

Application of Finite-Element Theory to Airplane Configurations

R. G. Bradley* and B. D. Miller†
General Dynamics Corporation, Fort Worth, Texas

Some applications of numerical lifting-surface theory for the calculation of steady subsonic and supersonic flow over complete airplane configurations are presented. Major emphasis is placed on the evaluation of a numerical finite-element theory as an aerodynamic loads prediction method for complex airplane geometries. Experimental pressure distribution data are compared with the distributed-singularity solutions in order to demonstrate the applicability as well as some of the limitations of the linearized theory for actual airplanes. The results reveal that the numerical theory can be useful for aerodynamic evaluation of complex airplane configurations. Proper usage of the theory, however, does require an understanding of the aerodynamics of the configuration and the limitations of the numerical method.

Nomenclature

b = wing span
c = wing chord
C_L = lift coefficient
C_M = pitching moment coefficient
C_p = pressure coefficient
l = body length
M = Mach number
x = chordwise distance
y = spanwise distance
α = angle of attack
Λ_{LE} = leading-edge sweep angle
θ = body meridian angle measured clockwise from vertical

Introduction

AERODYNAMIC design and evaluation has relied for many years on classic aerodynamic theories for thin wings and slender bodies, salted heavily with empirical factors, and on extensive wind-tunnel testing. In recent years, however, the appearance of highly efficient digital computers has opened the door for renewed emphasis on development of sophisticated analytical aerodynamic theories. The extent of this renewed emphasis on numerical methods was perhaps best illustrated at a recent NASA conference on analytical methods in aircraft aerodynamics,[1] where the development and results of numerous sophisticated computer programs were featured.

Presented as Paper 70-192 at the AIAA 8th Aerospace Sciences Meeting, New York, January 19–21, 1970; submitted February 19, 1970; revision received November 9, 1970. This research was supported by General Dynamics Independent Research and Development funds.

* Design Specialist. Member AIAA.
† Project Aerodynamics Engineer. Member AIAA.

The authors have evaluated several numerical lifting surface theories for a variety of wing configurations by comparison of theoretical results with experimental data.[2] The numerical methods include both collocation and finite-element theories, which were compared with each other, where applicable, and with experimental data. These comparisons reveal that the several numerical methods based on linearized theory give essentially equivalent results for wing-alone problems.

While wing design is an important part of the design process, the airplane designer is still faced with a multitude of problems which cannot be treated within the framework of wing-alone theory. Interfering flowfield effects are of paramount importance for practical airplane design, where the acid test for theory is agreement with wind-tunnel test. Wing-body interaction and blending, flowfield specification at inlet locations, rigid aerodynamic loading on components, and nacelle or store effects on the vehicle are some problems of concern. One analytical tool for attacking these problems is finite-element theory. Large computing facilities in common usage today make the distributed-singularity approach (and the associated-matrix-inversion requirements) feasible for complex configurations.

Application of theory to practical airplane design must be predicated on a basic understanding of the limitations of the theory and on an experimentally confirmed level of confidence. It is the purpose of this paper to examine one of the currently available finite-element methods in the context of aerodynamic-loads prediction for real airplanes.

Theory

The finite-element theory of Woodward[3] forms the basis for the following applications. The numerical method is an extension by Woodward and Hague[4] of a supersonic wing-

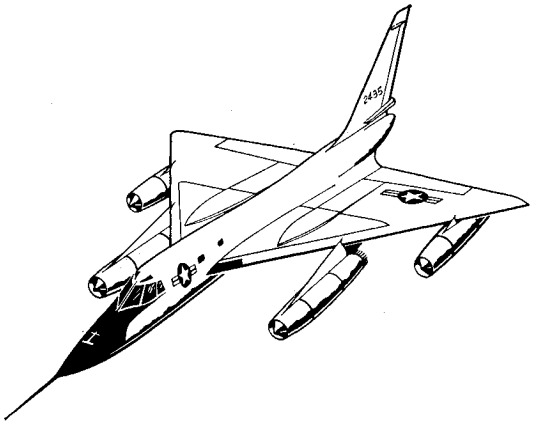

Fig. 1 B-58 configuration.

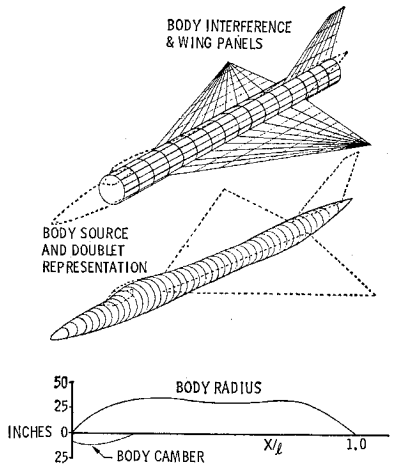

Fig. 2 B-58 wing-body description.

body program developed for the NASA/Ames Research Center[4] to include more complex geometry and to provide subsonic flow solutions.

Wings and bodies are represented by distributions of source, doublet, and vortex singularities whose strengths are adjusted to satisfy the flow-tangency boundary conditions required by the geometry of the particular configuration. The effects of body volume, incidence, and camber are represented by line sources and doublets distributed along the body axis; the effects of wing thickness are simulated by planar source distributions; and the effects of wing camber, twist, and incidence are given by planar vortex distributions. The interference effects of other surfaces on the bodies are provided by additional vortex distributions on panels near the body surface.

The numerical method is implemented by a digital computer program that allows combinations of up to 10 wings and 10 bodies. A maximum of 200 body interference panels and 200 wing panels is allowed. The program provides pressure distributions, integrated force and moment data, and flowfield calculations for specified geometry. In addition, design capability is provided in the generation of optimum wing surface warp for a specified lift constraint, and in the generation of wing surface warp necessary to support a specified pressure distribution.

Applications

The finite-element theory has been shown to be valid for wing-along cases and for simple wing-body configurations.[2,3,5] Here, attention is focused on results for actual airplanes where the application of theory is not so straightforward. Satisfactory representation of real airplane configurations with their usual noncircular body and nacelle cross-sectional shapes often requires keen judgment on the part of the aerodynamicist. Further, the applicability of linear theory to complex interfering flow situations has not yet been firmly established. The following sections present some applications of the numerical method of Woodward and Hague to the B-58 and F-111 airplane configurations. Comparisons are made with wind-tunnel pressure and force data in order to indicate the utility and limitations of the theoretical method.

B-58 Comparisons

The B-58 is a four-engine, supersonic, bomber configuration (Fig. 1). The wing is a delta planform with conical camber and a NACA 0004.08-63 airfoil section.

Wing body

The basic wing-body is a slender configuration well suited to linearized-theory assumptions. The mathematical description of the configuration is shown in Fig. 2. Body radius and camber are specified at 45 stations to establish the line source and doublet strengths to simulate the body. An obvious discrepancy in the fuselage representation may be noted in the vicinity of the canopy. The body interference-panel cylinder is defined by 96 panels. The wing and vertical tail are defined by 80 and 28 panels, respectively. Values of camber and thickness slopes are specified for each panel.

Computed pressure distributions on the wing are compared with experimental data in Fig. 3. Agreement is seen to be generally good for both the subsonic and supersonic flow conditions. The poorest agreement is noted at outboard stations near the tip for both flow conditions. The conical camber in the B-58 wing results in very large camber slopes near the tip. Those slopes may account, in part, for the accuracy deterioration of the linearized theory as the wing tip is approached. However, similar results are reported[2] for an arrow-wing example where the camber slopes are not excessive near the tip.

Nacelles

Several possibilities are apparent for adding the nacelles to the configuration within the framework of the finite-

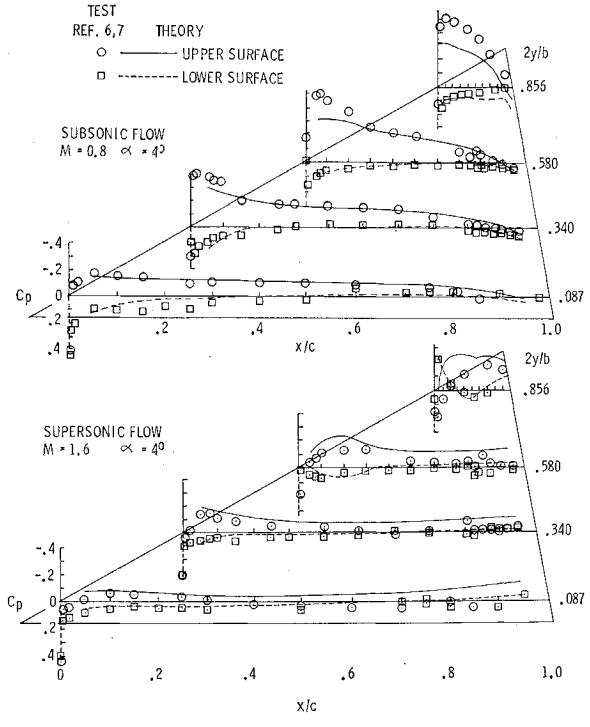

Fig. 3 B-58 wing pressures—nacelles off.

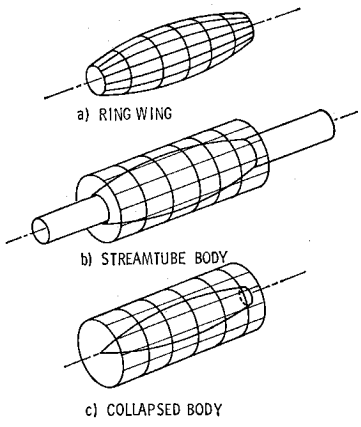

Fig. 4 Nacelle representations.

element theory. At first, one might expect that a ring-wing representation for the nacelle holds the most promise (Fig. 4a). An evaluation of this alternative was made by investigating the concept for an isolated duct. The results of these nacelle-alone studies indicate that, for slender ring wings representative of nacelles, an excessive number of panels are required to give a realistic external pressure distribution.

Another alternative represents the nacelle as a body of revolution with a cylindrical streamtube extending from the forward and aft ends of the nacelle to locations well out of flowfield influence (Fig. 4b). A disadvantage of this concept is that the streamtube must be rotated as angle of attack is changed in order to maintain alignment with the freestream. Still another possibility is to remove the internal flow area and collapse the nacelle thickness to the duct centerline to make a slender body, as shown in Fig. 4c.

The first alternative, the ring wing, was ruled out for the B-58 because of the large number of panels required. A brief study of the latter two concepts, with only the inboard nacelle on the wing, was made. The results, shown in Figs. 5–8, reveal several interesting facts. In Fig. 5, comparisons are presented of the pressures at two angular positions on the inboard nacelle. Results for both the streamtube and slender-nacelle approximations are shown. Only small differences are noted in the solutions, and both agree very well with data taken on the B-58 nacelles. Wing data at two nearby span stations are shown in Fig. 6. The pressures for the slender-body representation are somewhat smoother than for the streamtube case. It is noted that the B-58 experimental data shown in Figs. 5 and 6 were taken with all four nacelles on.

The interference pressures near the nacelles were found to be dependent on the number of panels positioned on the nacelle interference cylinder. This effect is illustrated in Figs. 7 and 8, where wing and nacelle pressures, respectively,

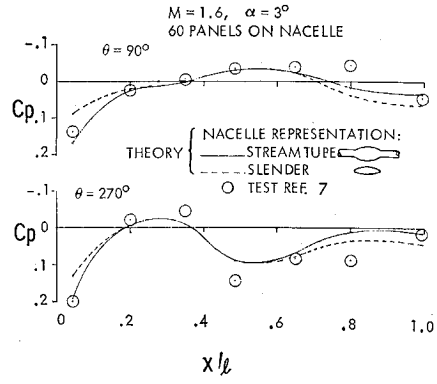

Fig. 5 Nacelle representation effect—nacelle pressures.

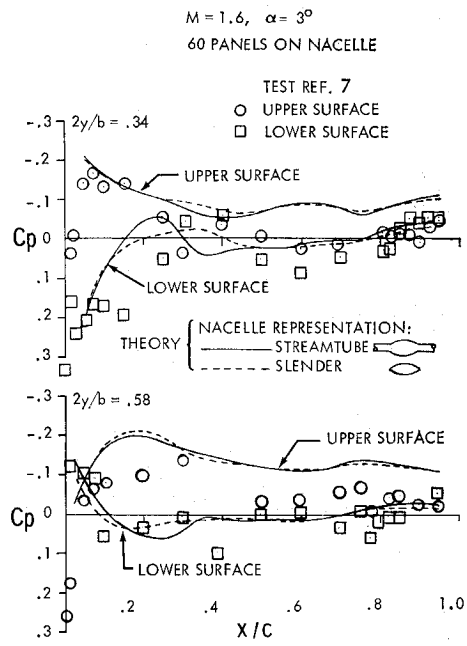

Fig. 6 Nacelle representation effect—wing pressures.

are compared for the calculations made with and without interference panels placed around the nacelles. The no-panel case, of course, results in body-alone pressures on the nacelle (caused by only the nacelle sources and doublets) and in first-order interference effects of the nacelle sources and doublets on the wing.

A significant difference in both the nacelle and wing pressures is noted between runs with 60 panels and with 180 panels. Figure 7 indicates that the solution for the increased number of panels gives wing pressures approaching very closely the pressure levels induced by the nacelle with no panels at all. Thus, it appears that if only the effect of the nacelle on the wing were desired it would be better to run with no panels on the nacelle than with too few panels. Of course the body panels are necessary for accurate nacelle pressure calculations in the presence of the wing.

Total configuration

The wing pressures for the complete B-58 configuration are shown in Fig. 9. Based on the studies summarized above, the nacelles-on configuration has slender nacelles with no body panels and has pylons with thicknesses specified.

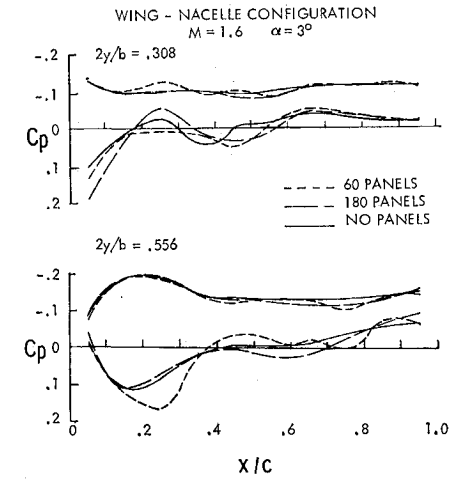

Fig. 7 Nacelle panel effect—wing pressures.

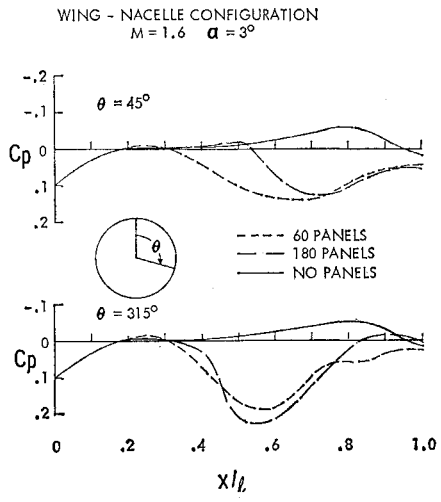

Fig. 8 Nacelle panel effect—nacelle pressures.

The wing and fuselage are defined as in the previous nacelles-off configuration. Comparison of the predicted pressures with the experimental data indicate generally good agreement. Pressures on the lower surface, where interference effects are most severe, are predicted exceptionally well. Leading-edge pressures at subsonic speeds are somewhat underpredicted. This underprediction may be a result of the coarse thickness slope definition near the leading edge (large chordwise panel spacing).

Fuselage pressures for a few typical meridian angles are shown in Fig. 10 for subsonic and supersonic flow. The trends are generally correct. Obviously, pressures in the vicinity of the canopy are not correct.

The lift and pitching-moment curves are given in Fig. 11 for the complete B-58 configuration. Agreement between theory and experiment is good.

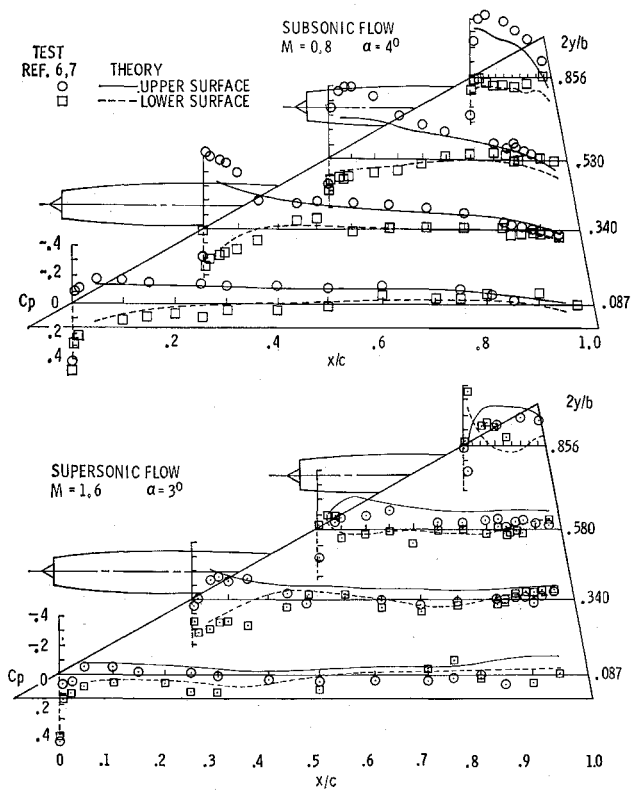

Fig. 9 B-58 wing pressures—nacelles on.

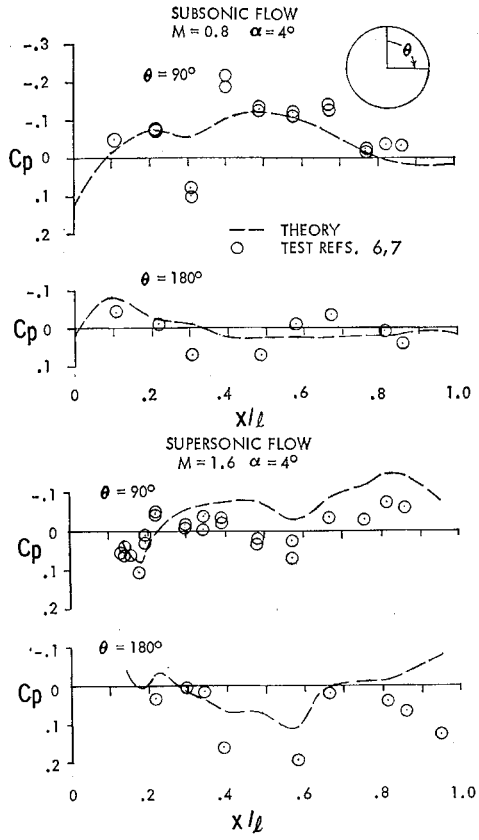

Fig. 10 B-58 fuselage pressures—nacelles on.

F-111A Comparisons

Some results are presented for the F-111A variable-sweep fighter-bomber. The F-111A example is a particularly stringent test for the linearized theory in that the configuration is not slender and the fuselage is far from a circular cross section, particularly at the aft locations where the nacelles are located. Preliminary simple representations have been employed and the results are presented.

Low-speed configurations

The entire low-speed configuration is represented by a single lifting surface, as shown in Fig. 12. A total of 195 panels is used. Thickness and camber slopes are specified on the wing panels. The fuselage is approximated by specifying appropriate thickness and camber slopes on those panels representing the fuselage.

The results of the finite-element calculation are compared with pressure data on the wing and tail surfaces in Fig. 13. The data were obtained on a $\frac{1}{12}$-scale wind-tunnel pressure model. The agreement between theory and experiment is very good. The upper and lower fuselage pressures ($\theta = 0°$ and $\theta = 180°$) are compared with the computed pressures

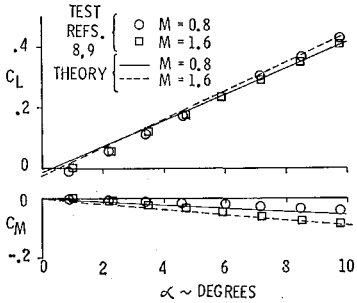

Fig. 11 B-58 lift and moment curves.

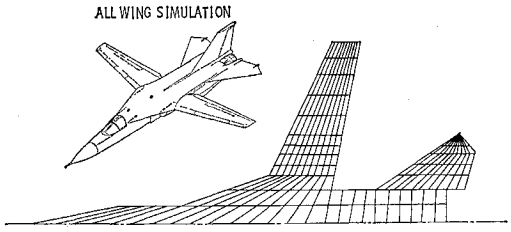

Fig. 12 F-111A lifting-surface approximation.

for the simulated fuselage in Fig. 14. The trends in the data are predicted very well.

Supersonic configurations

Another approximation for the configuration is considered for the supersonic case. The body is approximated by a body of revolution defined by the cross-sectional area of the actual fuselage, excluding the nacelle-inlet areas. Figure 15 shows the representation schematically. The wing, glove, and tail are defined by 172 panels, and an interference cylinder consisting of 90 panels surrounds the body.

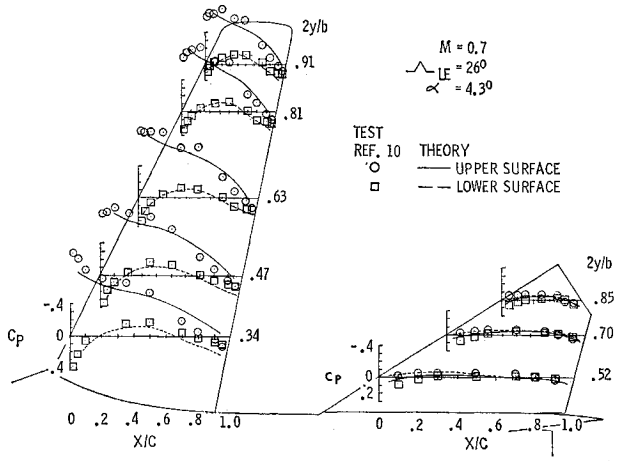

Fig. 13 F-111A wing and horizontal tail pressures.

The resulting wing and tail surface pressure distributions are compared with test data in Fig. 16. Again, very good agreement is noted except on the outboard sections of the horizontal tail, where the upper-surface pressures are underpredicted. Surface pressures on the fuselage are compared with experiment in Fig. 17. The agreement is surprisingly good in view of the crude fuselage approximation. The

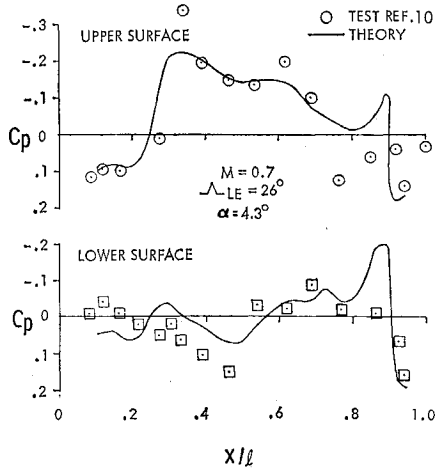

Fig. 14 F-111A fuselage pressures.

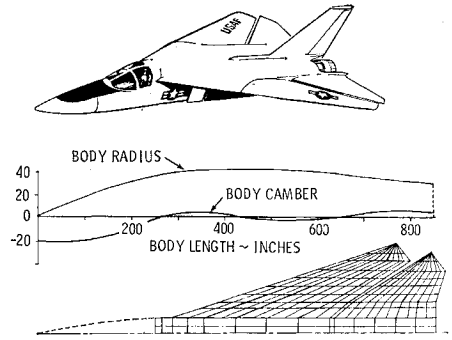

Fig. 15 F-111A supersonic configuration description.

theory appears to aptly predict the interference effects on the body.

Lift and moment curves for both the subsonic and supersonic configurations are shown in Fig. 18. The lifting-surface representation of the low-speed configuration is noted to overpredict the moment somewhat. On the other hand, the subsonic lift and the supersonic lift and moment data are predicted very well by the theory.

In the preceding discussion, only first-pass approximations have been used in representing the F-111A with distributed

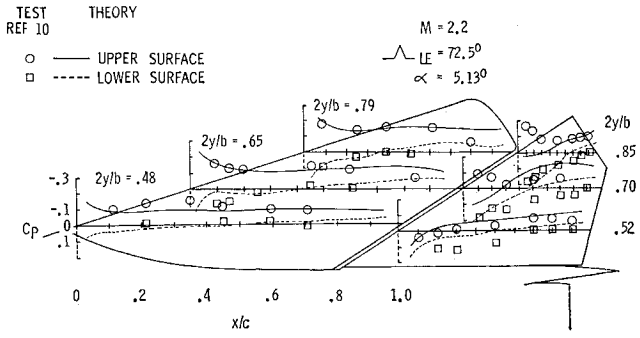

Fig. 16 F-111A wing and horizontal tail pressures.

singularities within the framework of the Woodward and Hague method. Quite obviously much more sophisticated techniques could be used to improve the accuracy. Nevertheless, it is felt that the preliminary findings point to a significant potential in the finite-element method.

Concluding Remarks

The potential of distributed-singularity techniques as an aerodynamic evaluation tool for practical, complex airplane configurations has been demonstrated. It is not unreasonable to expect that greater sophistication in the numerical methods

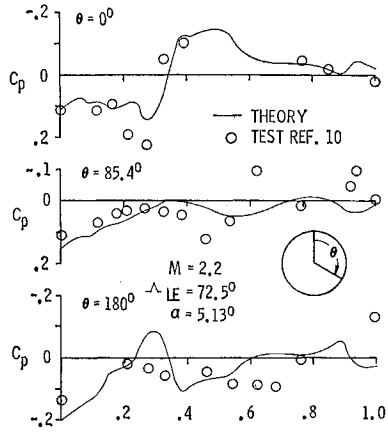

Fig. 17 F-111A fuselage pressures.

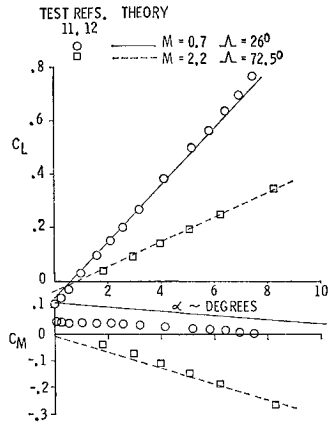

Fig. 18 F-111A lift and moment curves.

is feasible, with emphasis perhaps on nonlinear boundary conditions. The B-58 solutions required one hour of computer time on an IBM 360 model 65. Computers with greater speed, storage capacity, and accuracy are presently available, and certainly next-generation computing equipment will be suitable for expanded finite-element applications.

On the other hand, it is noted that usage of finite-element theories at the present time is far from a push-the-button task. Aerodynamic insight and an understanding of the theory limitations are required to accurately apply the numerical method to complex configurations. Much is yet to be learned about effects of interference-panel location, nonsymmetric body representation, and interpretation of the resulting flowfield.

The question of drag has been omitted from the present discussion. Interpretation of the results of lifting-surface theory with respect to aerodynamic drag remains a question of some uncertainty in the subsonic speed regime. For supersonic flows, the finite-element theory provides drag due to lift, which contributes to a drag buildup technique as described by Baals et al.,[13] for example. Zero-lift wave drag is given by the theory at supersonic speeds, perhaps with not as great accuracy as the well-established far-field (area-rule) theory. However, at subsonic speeds, the present finite-element method does not account for leading-edge suction for a round-nosed airfoil in a real flow. Several theoretical approaches to the leading-edge suction problem are possible but are beyond the scope of the present paper.

References

[1] *Analytical Methods in Aircraft Aerodynamics*, SP-228, NASA, Moffett Field Calif., Oct. 1969.

[2] Bradley, R. G. and Miller, B. D., "Lifting Surface Theory-Advances and Applications," AIAA Paper 70-192, New York, 1970.

[3] Woodward, F. A., "Analysis and Design of Wing-Body Combinations at Subsonic and Supersonic Speeds," *Journal of Aircraft*, Vol. 5, No. 6, Nov.-Dec. 1968.

[4] Woodward, F. A. and Hague, D. S., "A Computer Program for the Aerodynamic Analysis and Design of Wing-Body-Tail Combinations at Subsonic and Supersonic Speeds, Volume I: Theory and Program Utilization," Rept. ERR-FW-867, Feb. 1969, Fort Worth Div., General Dynamics Corp.

[5] Carmichael, R. L. and Woodward, F. A., "An Integrated Approach to the Analysis and Design of Wings and Wing-Body Combinations in Supersonic Flow," TN D-3685, Oct. 1966, NASA.

[6] Walker, C., "Summary Report of Wind Tunnel Tests on a 1/17-Scale Pressure Model of the Project MX-1964 Airplane at the 10-Foot Transonic Tunnel of WADC," Rept. FZT-4-102, 22 Sept. 1955, Convair-Fort Worth Division.

[7] Wilkerson, C., Jr., "Summary Report of Supersonic Pressure Distribution Tests on the 1/17-Scale Pressure Model of the Project MX-1964 Airplane (AAL 124)," Rept. FZT-4-085, Sept. 1955, Convair-Fort Worth Division.

[8] Bock, R. P., "Summary Report of a Subsonic Wind Tunnel Test on a 1/17-Scale Force Model of the Project MX-1964 Airplane (CWT Test 463)," Rept. FZT-4-131, April 1965, Convair-Fort Worth Division.

[9] Lawrence, W. J., "Project MX-1964 Subsonic and Supersonic Force Tests of a 1/17-Scale Model of the B-58 Airplane (AAL Test 122)," Rept. FZT-4-148, Sept. 1956, Convair-Fort Worth Division.

[10] Douglas, J., "Wind Tunnel Data Report, 1/12-Scale F-111 Rigid Loads Model at the Ames Research Center, Ames Test No. 81, GD/FW Test Nos. 74, 75, and 76," Rept. FZT-12-101, Nov. 1964, General Dynamics-Fort Worth Division.

[11] Reeves, R. W., "Wind Tunnel Data Report, 1/15-Scale F-111 Force Model No. 2, Cornell Aeronautical Laboratory 8′ Transonic Wind Tunnel, CAL Test G52-143, GD/FW Test No. 83," Rept. FZT-12-103, Oct. 1964, General Dynamics-Fort Worth Division.

[12] Wray, W. O., Jr., "Wind Tunnel Data Report, 1/24-Scale F-111A Force Model Speed Brake Test, NASA Langley Research Center Test Nos. 141 and 142," Rept. FZT-12-166, June 1967, Fort Worth Division.

[13] Baals, D. D., Robins, A. W., and Harris, R. V., Jr., "Aerodynamic Design Integration of Supersonic Aircraft," AIAA Paper 68-1018, Philadelphia, Pa., 1968.